

# Optimization on Planning of Trajectory and Control of Autonomous Berthing and Unberthing for the Realistic Port Geometry

Yoshiki Miyauchi<sup>a,\*</sup>, Ryohei Sawada<sup>a,b</sup>, Youhei Akimoto<sup>c,d</sup>, Naoya Umeda<sup>a</sup> and Atsuo Maki<sup>a,\*</sup>

<sup>a</sup>Department of Naval Architecture and Ocean Engineering, Graduate School of Engineering, Osaka University, 2-1 Yamadaoka, Suita, Osaka 565-0971, Japan

<sup>b</sup>National Maritime Research Institute, 6-38-1, Shinkawa, Mitaka, Tokyo 181-0004, Japan

<sup>c</sup>Faculty of Engineering, Information and Systems, University of Tsukuba, 1-1-1 Tennodai, Tsukuba, Ibaraki 305-8573, Japan

<sup>d</sup>RIKEN Center for Advanced Intelligence Project, 1-4-1 Nihonbashi, Chuo-ku, Tokyo 103-0027, Japan

## ARTICLE INFO

**Keywords:**

Autonomous Berthing /Unberthing  
Trajectory Planning  
Optimization  
CMA-ES  
Collision Avoidance  
Ship Domain

## ABSTRACT

To realize autonomous shipping, autonomous berthing and unberthing are some of the technical challenges. In the past, numerous research have been done on the optimization of trajectory planning of berthing problems. However, these studies assumed only a simple berth and did not consider obstacles. Optimization of trajectory planning on berthing and unberthing in actual ports must consider the spatial constraints and maintain sufficient distance to obstacles. The main contributions of this study are as follows: (i) a collision avoidance algorithm based on the ship domain which has variable size by the ship speed is proposed, to include the spatial constraints to optimization; (ii) the effect of wind disturbance is taken into account to the trajectory planning to make a feasible trajectory based on the capacity limit of actuators; (iii) showing that the optimization method for berthing is also eligible for the unberthing, which has been almost neglected; (iv) waypoints are included to the optimization process, to make optimization easier on practical applications. The authors tested the proposed method on two existing ports. The proposed method performed well on both the berthing and the unberthing problem and optimized the control input and the trajectory while avoiding collision with the complex obstacles.

## 1. Introduction

Realizing autonomous ship navigation, autonomous berthing is one of the major technical challenges. Operations such as berthing and unberthing at a narrow fairway are the most stressful for the navigator. This is because “*The difficulty is not only due to the increase in the number of maneuvering measures, but also because the ship is forced to maneuver in a severe surrounding environment, including spatial constraints such as breakwaters and berths, reduced maneuverability due to low-speed navigation, and increased effects of wind and currents.*” (Seta et al., 2004) Thus, berthing and unberthing are relatively difficult than that of navigation of open-sea. Thus automation of these kinds of maneuvering is useful not only from the viewpoint of reducing the operational cost but also from reducing the workload on the navigator.

In solving the online control of the autonomous berthing, it is effective to use the predefined trajectory and control input as a reference for tracking control obtained by the optimization problem. The process to generate the predefined trajectory is called trajectory planning. In this paper, we defined that trajectory as time series of state of the ship, including geometric paths, with some or all dynamic constraints of the ship, by referring to the definition of Vagale et al. (2021): “*path planning is typically defined within purely geometric space, whereas trajectory planning, or trajectory generation, involves geometric paths endowed with tempo-*

*ral properties, e.g., to incorporate dynamics.*” Trajectory planning is generally difficult to directly apply to the control algorithm due to the computation requirements, which is longer than the computation time required for real-time control, caused by the non-linearity of the maneuvering motion. However, whether using classical control such as PID control or a black box approach such as neural networks, if this reference trajectory and control can be generated using a mathematical model of the maneuvering motion, it is possible to obtain feasible control that is optimized for some metrics such as time, while satisfying constraints based on the ship’s maneuvering performance such as actuator capacity limits.

### 1.1. Related Research

In the past, numerous research have been done on the optimization of trajectory planning and control of berthing problems (Hasegawa and Kitera, 1993; Ahmed, 2015; Maki et al., 2020a,b). However, most of these studies have assumed only a simple straight berth and do not consider surrounding obstacles. To perform berthing and unberthing in actual ports, it is necessary to avoid static obstacles such as bridge piers, berths other than the destination and anchored ships, as well as moving obstacles such as passing ships.

Only a few research have included the complex geometric constraints of the port to trajectory planning of berthing. Those research have used a two-stage method which combined the path planning using graph search and optimal control problem solver for trajectory generation: optimization of trajectory planning with polygonal constrains which combined the graph-search and convex optimization (Martinsen

\*Corresponding author

yoshiki\_miyauchi@naoe.eng.osaka-u.ac.jp (Y. Miyauchi);  
maki@naoe.eng.osaka-u.ac.jp (A. Maki)

et al., 2019, 2020); combined the hybrid A\* search algorithm as an initial guess to an optimal control problem solver under the external disturbance (Bitar et al., 2020); the combination of lattice-based motion planning and receding horizon improvement, creating initial trajectory using the lattice-based motion planning which transforms the optimal control problem to classical graph search problem and optimization based improvement of the initial trajectory using receding horizon improvement while the ship maintaining a fixed safe distance to obstacles (Bergman et al., 2020). These research have adopted the two-stage method, which discrete the continuous state space to apply graph search which obtains an initial guess and optimize the initial guess with an optimization problem solver. These research also have only considered the constant radius of safety region to the obstacle. Trajectory planning on other kinds of restricted waters have been reported on: global trajectory planning and collision avoidance of an autonomous surface vessel at narrow ferry passage by safety region and collision region around moving and static obstacles with applying the hybrid dynamic window method (Serigstad et al., 2018); Navigation in restricted channels using reinforcement learning was done by Amendola et al. (2020).

On the optimization of berthing and unberthing trajectory, it is important to consider whether the trajectory avoids the obstacle and whether the trajectory is separated from the obstacle by a sufficient distance for safety. The problem of how much distance a ship should keep from obstacles, was investigated by Fujii and Tanaka (1971) in the 1970s as *effective domain*; and followed by Goodwin (1975), which defined *ship domain* as “the effective area around a ship which a navigator would like to keep free with respect to other ships and stationary objects.” Since then, various models have been proposed and applied to the collision avoidance method. Szlapczynski and Szlapczynska (2017) provides a comprehensive review of these ship domain models. However, many models did not address the geographical constraints because the ship domain was mainly used to represents the safe distance between ships. Effective domain at restricted waters was proposed by Yamanouchi and Fujii (1972) based on observation of navigation outside the port of Yokohama, Japan, and showed that in restricted waters, the ship domain is smaller than open seas, which about three-fourths in the longitudinal direction and about half in the width direction. Ship domain based on traffic at strait proposed by Wang and Chin (2016) that is proportional to the ship length and speed. The coefficients are determined based on the Vessel Traffic Information System (VTIS) database of ships transiting the Singapore Strait by using a genetic algorithm. Pietrzykowski (2008) proposed a ship fuzzy domain with the shape of the narrow fairway as a parameter. Hansen et al. (2013) proposed the ship domain on restricted waters based on AIS data measured on the Fehmarnbelt between Denmark and Germany and Jensen et al. (2013) followed that work by estimating the traffic separating scheme’s efficiency on the bridge pier of Fehmarnbelt. However, in our literature survey, the ship domain designed to apply to berthing

or unberthing problems cannot be found.

## 1.2. Objective and Scope

The objective of this study is to include several major factors necessary for applying optimization of trajectory planning on both berthing and unberthing to practical application, such as spatial constraints and external disturbance. Trajectory planning on unberthing has not been focused on previous research compare to berthing; however, it is equally important to realize the fully autonomous ship. The main contributions of this study are as follows: (i) a new collision avoidance algorithm based on the ship domain which has variable size by the ship speed was proposed, to include the spatial constraints to optimization of trajectory planning; (ii) effect of wind disturbance was taken into account to the trajectory planning to make a feasible trajectory based on the capacity limit of actuators; (iii) showing that the optimization method for berthing is also eligible for the unberthing, which has been almost neglected on the field on trajectory planning; (iv) waypoints are included to the optimization process, to make optimization easier on practical applications. Major environmental conditions related to berthing and unberthing consist of wind, wave, and current. However, disturbance caused by wave and current were neglected in this study, assuming that the vessel enters a port sheltered by breakwaters.

By adding the idea of ship domain to the collision avoidance algorithm, the proposed method enables the search for a trajectory that maintains an appropriate distance from the obstacle. In this study, the obstacle was limited to a static obstacle, but the algorithm can be extended to a dynamic obstacle.

This study extends the study of Maki et al. (2020a) the Co-variance Matrix Adaption Evolution Strategy (CMA-ES) for the optimization process. The subject ship is a relatively large single-rudder, single-propeller ship with side thrusters, which can berth and unberth without assistance by tug boats. The proposed method requires only the initial and desired end state, control constraints, and spatial constraints of obstacle geometry as computational conditions. To validate the proposed algorithm, we also performed calculations on multiple ports.

The rest of the paper is organized as follows: Section 2 describes the optimization method of trajectory planning and mathematical modeling of maneuver. The optimization method contains the collision avoidance algorithm, which is newly proposed in this study; Section 3 shows the test result on trajectory planning using a newly introduced optimization scheme with a collision avoidance algorithm. Section 3 also describes the geometry of ports which served as test cases; In Section 4, a discussion on the results shown in the previous section and future works are shown; Finally, section 5 concludes the study.

## 2. Method

In this study, berthing and unberthing are modeled as 3 degrees-of-freedom problem. The coordinate systems are

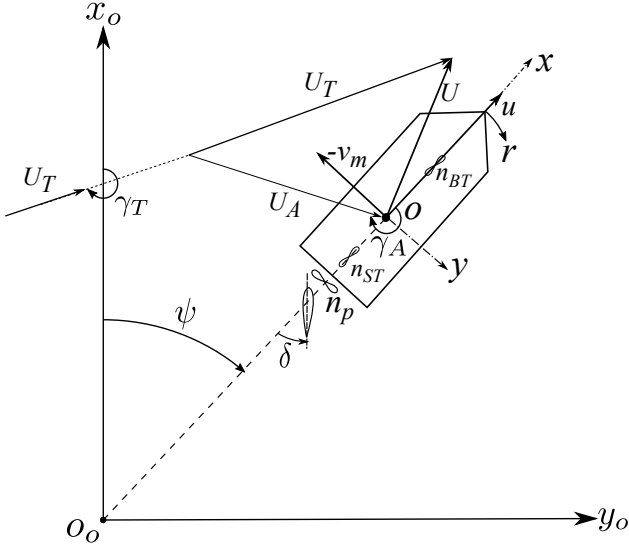


Fig. 1: Coordinate System

space-fixed system  $o_0 - x_0y_0$  and ship-fixed system  $o - xy$  which has its origin on midship. The origin of  $o_0 - x_0y_0$  was set as the position of midship at designated berthing point or the start point of unberthing, true-north direction as the positive direction of  $x_0$ , east direction as the positive direction of  $y_0$ . Fig. 1 shows the coordinate systems in this study. State vector is  $\mathbf{x} = (x_0, u, y_0, v_m, \psi, r)^T \in \mathbb{R}^6$ , where  $u, v_m$  are the velocity of  $o - xy$  system. The vector of control input is  $\mathbf{u} = (\delta, n_p, n_{BT}, n_{ST})^T$ .  $\delta, n_p, n_{BT}, n_{ST}$  represent the rudder angle, the revolution of propeller, the bow thruster and the stern thruster, respectively. The positive direction of the rudder angle was set to the direction in which the heading angle  $\psi$  increase by steering, positive rotation of propeller was set to the advancing direction, positive rotation of side thrusters was set to the direction which the induced force work to move the ship to the positive direction of ship-fixed coordinate  $y$ .

Wind disturbance was considered as external force  $\boldsymbol{\omega}$ , which consist by the true wind direction and true wind speed  $\boldsymbol{\omega} = (\gamma_T, U_T)^T$ . However, due to the ship's maneuver, an apparent wind affects as the actual force acting on the hull. Hence the apparent wind was computed inside the mathematical model of maneuvering. The zero direction of true wind direction  $\gamma_T$  was set to the direction in which the wind blows from the positive direction to the negative direction of  $x_0$ .

## 2.1. Optimization of Trajectory planning

### 2.1.1. Objective Function

In this study, the berthing and unberthing problems were modeled as time-minimizing problem. The state equation shown is Eq. (1):

$$\dot{\mathbf{x}}(t) = \mathbf{f} \{ \mathbf{x}(t), \mathbf{u}(t), \boldsymbol{\omega}(t) \}. \quad (1)$$

On the berthing and unberthing problem, the initial and end state are given. By expanding the objective function  $J$  pro-

posed by Maki et al. (2020a),  $J$  in this study is:

$$J = w_c \cdot C + t_f \cdot \sum_{i=1}^6 w_{\dim,i} \left( x_{\text{tol},i}^2 \mathbf{1}_{\{|x_{\text{des},i} - x_i(t_f)| \leq x_{\text{tol},i}\}} + w_{\text{pen}} (x_{\text{des},i} - x_i(t_f))^2 \mathbf{1}_{\{|x_{\text{des},i} - x_i(t_f)| > x_{\text{tol},i}\}} \right), \quad (2)$$

where the difference  $x_{\text{des},5} - x_5(t_f)$  in angle should be treated as a value in  $(-\pi, \pi]$  by taking into account the minimum difference angle and  $\mathbf{1}_{\{A\}}$  is the indicator function that is 1 if  $A$  is true and 0 otherwise. Here, subscript  $i = 1, 2, \dots, 6$  means a related term to the  $i$ -th component of the state vector. The first term of  $J$  is the penalty term for the collision with obstacles, and the second term is for satisfying the desired end state condition.  $\mathbf{x}_{\text{int}}$  and  $\mathbf{x}_{\text{des}}$  are the vectors of given initial state and the desired end state.  $\mathbf{x}_{\text{tol}}$  is the tolerance vector to the difference between the actual and desired end state, which was introduced to prevent  $t_f$  from increase due to the pursuit with excessive precision of the end state during the optimization process, same as the previous study (Maki et al., 2020a).

In the case of unberthing,  $u$  does not need to be in the certain range of tolerance, instead it should be better just above the certain exit speed. Thus, for the unberthing case, the condition of indicator function of Eq. (2) replaced by  $u(t_f) \geq x_{\text{tol},2}$ .  $w_{\text{pen}}$  is the penalty coefficient when the actual end state not satisfy the  $\mathbf{x}_{\text{tol}}$ ,  $w_{\text{dim}}$  is the collection vector for state vector components which have different dimensions. On the second term,  $C$  is the collision penalty function and  $w_c$  is the weight coefficient for collision penalty. Details of collision penalty function is shown on section 2.1.2. List of coefficient and  $\mathbf{x}_{\text{tol}}$  are shown on Table 1.

There is some discussion on how to configure  $\mathbf{x}_{\text{tol}}$ . On the berthing speed in Japanese ports, Murakami et al. (2015) proposed a regression equation based on measurement. However, their study was conducted from the perspective of allowable values in port design, not from how much the ship needs to slow down. On the heading angle, Roubos et al. (2017) analyzed 555 records of berthing of tankers, bulkers, and container ships in the port of Rotterdam and found that the approach angle to the berth at the moment of impact is less than  $1.5^\circ$ . The tolerance  $\mathbf{x}_{\text{tol}}$  was set based on the tolerance values of the state at the time of berthing in these previous studies. The velocity component of  $\mathbf{x}_{\text{tol}}$  was calculated from the regression equation for berthing velocity  $V$  which covers 90% of the measured data (Murakami et al., 2015):

$$V = 0.279 \cdot GT^{-0.114}, \quad (3)$$

where  $GT$  is the gross tonnage and was assumed as a ferry of approximately 10,000 tons, which operated on the subject port shown on section 3.1. The tolerance of  $\psi$  was set to  $\mathbf{x}_{\text{tol},5} = 1.0^\circ$ , which is slightly smaller than the maximum value in Roubos et al. (2017). The position's tolerance was set to 1.0m, which is small enough for the ship's length.

During the optimization, the optimization method searches for a combination of the time series  $\mathbf{u}(t)$  and  $t_f$  that

**Table 1**  
list of weight coefficients and tolerance vectors of end state

Parameter	Value	
Condition	Berthing	Unberthing
$\mathbf{x}_{tol}$	(1.0m, 0.1m/s, 1.0m, 0.1m/s, 1.0°, 0.0764°/s) <sup>T</sup>	(1.0m, 0.1m/s, 1.0m, 0.0m/s, 1.0°, 0.764°/s) <sup>T</sup>
$w_{pen}$		$1.0 \times 10^4$
$w_{dim}$	$(1/w_L^2, 1/w_U^2, 1/w_L^2, 1/w_U^2, \pi^2, w_L^2/w_U^2)^T$	
$w_C$		$1.0 \times 10^{10}$
$w_L$		$0.1L_{pp}$
$w_U$	$\mathbf{x}_{init,2}/2$	$\mathbf{x}_{des,2}/2$

**Table 2**  
Minimum and maximum of end time  $t_f$  and control inputs

Parameter	Value
$t_{f,min}$ (s)	630
$t_{f,max}$ (s)	2250
$ \delta_{max} $ , (degree)	35
$ n_{p,max} $ , (rps)	2.08
$ n_{BT,max} $ , (rps)	4.24
$ n_{ST,max} $ , (rps)	4.24

minimizes Eq. (2). The time series of the control input is kept constant during the period of  $t_c = 90$  s to prevent frequent input changes and to keep the number of variables to be searched finite. Hence time series of control inputs is discretized into  $m$  segments. Thus the variable  $\mathbf{X}$  to be optimized is follows:

$$\mathbf{X} \equiv (t_f, \delta_1, \dots, \delta_m, n_{p,1}, \dots, n_{p,m}, n_{BT,1}, \dots, n_{BT,m}, n_{ST,1}, \dots, n_{ST,m})^T \in \mathbf{R}^{4m+1} . \quad (4)$$

In this study  $m = 25$ , hence the maximum time of simulation is 2250 seconds.

Finally, the optimization problem can be expressed as follows:

$$\begin{aligned} & \mathbf{X}_{opt} = \operatorname{argmin} J(t_f, \mathbf{u}) \\ & \text{subject to : } x(0) = x_{int} \\ & t_{f,min} \leq t_f \leq t_{f,max} \\ & |\delta(t)| \leq \delta_{max} \\ & |n_p(t)| \leq n_{p,max} \\ & |n_{BT}(t)| \leq n_{BT,max} \\ & |n_{ST}(t)| \leq n_{ST,max} . \end{aligned} \quad (5)$$

The optimized trajectory is driven by substituting the  $\mathbf{X}_{opt}$  to the mathematical model of maneuver. The minimum and maximum value on the exploration of  $\mathbf{X}$  are shown in Table 2. The limits were set to: the maximum rudder angle of common rudder system; the propeller revolution of advancing at 8 kn; a revolution which can induce the equivalent force of the lateral wind force at 30 m/s when using both of the bow and the stern thruster.

### 2.1.2. Collision avoidance Algorithm

In the previous research (Maki et al., 2020a), to avoid collision to the berth, the penalty function  $C$  was applied to the objective function by integrating the instantaneous penetration length of the vertex of the rectangle surrounding the ship:

$$C = \sum_{i=1}^4 \int_{P_i \in C_{berth}} |Y_i - Y_{berth}| dt , \quad (6)$$

where  $P_i$  is the four vertices of the surrounding rectangle,  $C_{berth}$  is the area inside the berth,  $Y_i$  denotes each  $y_0$  ordinate of  $P_i$  and  $Y_{berth}$  represents the  $y_0$  coordinate of the berth edge. This collision avoidance method has several limitations for practical use: it can deal with only one berth at a time; the edge of a berth must be parallel to the  $y_0$  direction; safety distance to obstacles, such as berths, breakwaters, buoys or anchoring vessels, is not considered.

To overcome these limitations, the authors proposed a new collision avoidance algorithm on this study. The overview of the proposed collision avoidance algorithm as follows: (i) to maintain sufficient distance to the obstacle, the idea of ship domain was introduced to collision avoidance algorithm; (ii) to simplify the algorithm, ship domain was represented by polygon which has vertices at the boundary of domain (hereinafter, these vertices called as ‘‘domain boundary vertices’’); (iii) to generate a trajectory with sufficient distance to obstacle, penetration value of ship domain by obstacle was added to objective function as penalty function on the optimization process. In addition, obstacles are represented by polygons to address multiple, arbitrary shape obstacles.

The proposed algorithm avoid the collision and maintain sufficient distance to obstacle by minimizing the penalty function  $C$ , which is computed from the penetration length of domain boundary vertex to the obstacle:

$$C = \int_0^{t_f} \sum_{i=n_{obstacle}} \sum_{j=n_v} c_{i,j}(t) dt , \quad (7)$$

where  $C$  is the summation of instantaneous penalty  $c_{i,j}(t)$  between  $i$ -th obstacle polygon  $S_{obstacle,i}$  and  $j$ -th domain boundary vertex  $P_j$ :

$$c_{i,j}(t) = \begin{cases} L_{penet,j} & : P_j \in S_{obstacle,i} \\ 0 & : P_j \notin S_{obstacle,i} \end{cases} . \quad (8)$$

Here,  $n_v$  and  $n_{\text{obstacle}}$  represents the total number of domain boundary vertices and obstacles,  $L_{\text{penet},i,j}$  is the penetration length of  $P_j$  to  $S_{\text{obstacle},i}$ , which computed from the length between  $P_j$  and nearest edge of  $S_{\text{obstacle},i}$  to  $P_j$ .

A trajectory which does not maintain safe passing distance is not suitable for practical use. For instance, when the channel or fairway is bent and safe passing distance is not applied like the rectangular point around the hull used in the previous study, the ship makes a turn very close to the obstacle to shorten the  $t_f$ . Such a trajectory may shorten time of berthing, but maneuvering by tracking it may cause discomfort and fear to passengers and nearby manned vessels in practical use. Besides, the trajectory passing near obstacles is not safe to be used as a reference because there is not enough margin to recover from a gust. Hence, to optimize the trajectory planning in a real port, an optimal trajectory should be searched among trajectories that keep a passing distance away from obstacles as a human captain does. Thus, in this study, the ship domain was applied to the collision avoidance algorithm.

There are two major factors to define the ship domain; the shape of the domain and its size. Regarding the shape of the domain, the shape was designed as an ellipse which has the length ratio of 3:2:1 from midship to the bow, stern, and both sides of a ship, respectively, by referring the research on minimum passing distance in harbor based on inquires to pilots and captains (Inoue et al., 1994). In terms of the size of the domain, to approach to the berth, the ship domain has to shrink its size to avoid interference between the ship domain and the berth. Moreover, the ship must slow down when maneuvering in the vicinity of obstacle; it is better to keep a longer passing distance due to the increase of minimum stopping distance with speed.

Hence, the  $P_i$ 's coordinate  $P_{i,x}$   $P_{i,y}$  are determined by the semi-major axis  $a$ , semi-minor axis  $b$  and angle  $\alpha_i$ :

$$(P_{i,x}, P_{i,y}) = (a \cos \alpha_i, b \sin \alpha_i) , \quad (9)$$

where

$$\begin{aligned} a &= L_x(U) + 0.5L_{pp} \\ b &= L_y(U) + 0.5B . \end{aligned} \quad (10)$$

Margin length  $L_x$  and  $L_y$  are the function of the resultant velocity  $U = \sqrt{u^2 + v_m^2}$ . Angle  $\alpha_i$  is equally spaced, and defined by the ship-fixed coordinate system  $o-xy$ , with zero in the  $x$  direction and positive in the clockwise direction. the  $x$  direction margin length  $L_x$  has different lengths  $L_{x,L} > L_{x,S}$  in front and behind the hull. The length of the long side of the major axis is switched according to the forward speed's sign:

$$\begin{aligned} u \geq 0 : & \begin{cases} L_{x,L} \leftarrow \alpha_i \in (-\pi/2, \pi/2) \\ L_{x,S} \leftarrow \alpha_i \notin (-\pi/2, \pi/2) \end{cases} \\ u < 0 : & \begin{cases} L_{x,L} \leftarrow \alpha_i \notin (-\pi/2, \pi/2) \\ L_{x,S} \leftarrow \alpha_i \in (-\pi/2, \pi/2) . \end{cases} \end{aligned} \quad (11)$$

The  $L_{x,L}$ ,  $L_{x,S}$ , and  $L_y$  were constrained to certain maximum and minimum size to prevent the ship domain from becoming too large with increasing speed and to maintain a certain passing distance from obstacles even when the speed is low enough. To make the ship domain of this study applicable to the change of geometry of the port, the max. size of the ship domain was determined by the minimum passage width  $W$  in the port. We assumed a distance of  $0.25W$  from the edge of the obstacle in the width direction to pass the head-on situation. Combining with the length ratio of the ellipse's axes, we can obtain:

$$\begin{aligned} L_{x,\text{max},L} &= 0.75W - 0.5L_{pp} \\ L_{x,\text{max},S} &= 0.5W - 0.5L_{pp} \\ L_{y,\text{max}} &= 0.25W - 0.5B . \end{aligned} \quad (12)$$

On The minimum size, the shape is assumed to be front-to-back symmetric, to maintain sufficient margin on both bow and stern when rotating the ship, which may occur on the terminal phase of berthing and initial phase at confined berth.  $L_{y,\text{min}}$  was set to ship's width  $B$ , which is a typical stop point before mooring:

$$\begin{aligned} L_{x,\text{min}} &= 0.25L_{pp} \\ L_{y,\text{min}} &= B . \end{aligned} \quad (13)$$

Finally, The  $L_{x,L}$ ,  $L_{x,S}$ , and  $L_y$  express as follows:

$$L_{x,L}(U) = \begin{cases} L_{x,\text{max},L} & : U > U_{\text{max}} \\ L_{x,\text{min}} + \frac{(L_{x,\text{max},L} - L_{x,\text{min}})(U - U_{\text{min}})}{U_{\text{max}} - U_{\text{min}}} & : U_{\text{min}} \leq U \leq U_{\text{max}} \\ L_{x,\text{min}} & : U < U_{\text{min}} \end{cases} \quad (14)$$

$$L_{x,S}(U) = \begin{cases} L_{x,\text{max},S} & : U > U_{\text{max}} \\ L_{x,\text{min}} + \frac{(L_{x,\text{max},S} - L_{x,\text{min}})(U - U_{\text{min}})}{U_{\text{max}} - U_{\text{min}}} & : U_{\text{min}} \leq U \leq U_{\text{max}} \\ L_{x,\text{min}} & : U < U_{\text{min}} \end{cases} \quad (15)$$

$$L_y(U) = \begin{cases} L_y & : U > U_{\text{max}} \\ L_{y,\text{min}} + \frac{(L_{y,\text{max}} - L_{y,\text{min}})(U - U_{\text{min}})}{U_{\text{max}} - U_{\text{min}}} & : U_{\text{min}} \leq U \leq U_{\text{max}} \\ L_{y,\text{min}} & : U < U_{\text{min}} , \end{cases} \quad (16)$$

where linearly changing size with speed over the interval of speed  $U \in [U_{\text{min}}, U_{\text{max}}]$ . The limits in this study were set to  $[U_{\text{min}}, U_{\text{max}}] = [1\text{kn}, 6\text{kn}]$ .

Fig. 2 shows the ship domain and domain boundary vertices for  $W = 3.08 L_{pp}$ , which is the minimum passage width of the port of Nanko shown in section 3.1. The number of domain boundary vertices  $n_{\text{detect}} = 13$  in this study.

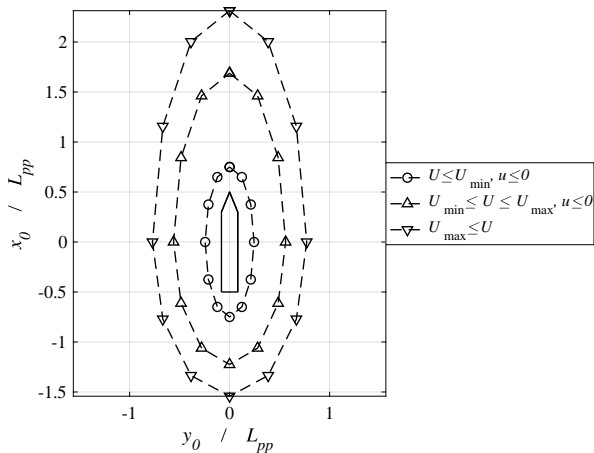


Fig. 2: domain boundary vertices on various speed

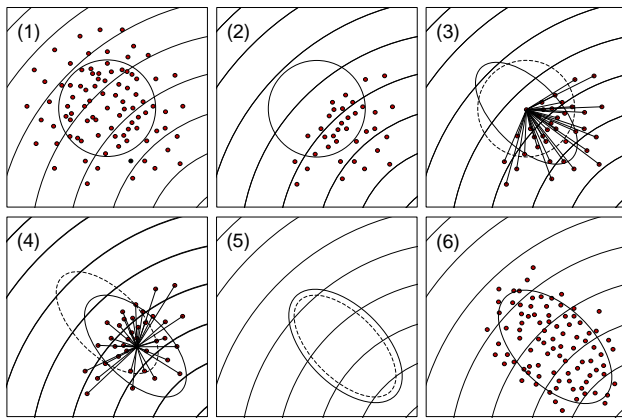


Fig. 3: Schematic presentation of the CMA-ES procedure including (1) generating multiple candidate solutions, (2) evaluating and ranking the solutions based on the objective function, (3) updating the covariance matrix, (4) shifting the center of the distribution to a weighted mean vector, (5) updating the step size and (6) generating multiple candidates in the next step. This figure duplicates Fig. 2 in the literature (Maki et al., 2020b)

### 2.1.3. Optimization Method: CMA-ES

As in the previous study (Maki et al., 2020a,b), covariance matrix adaption evolution strategy (CMA-ES) (Hansen, 2006) adapted to box constraints (Sakamoto and Akimoto, 2017) and with restart strategy (Auger and Hansen, 2005) was applied as optimization method. Fig.3 shows the procedure of optimization using CMA-ES. In previous research (Maki et al., 2020a), CMA-ES showed the capability to obtain a feasible solution on optimal berthing problem as a time-minimizing problem while taking into account the collision penalty to berth with simple geometry. In this study, the initial population size of CMA-ES is 20, and the max size is 240, while the population size was doubled when the restart occurred.

Table 3

Principal particulars of subject ship

Item	Value
Length between perpendicular: $L_{pp}$ (m)	150.0
Ship breadth: $B$ (m)	24.46
Ship draft: $d$ (m)	10.06
Diameter of propeller: $D_p$ (m)	4.20
Area of Rudder: $A_R$ (m <sup>2</sup> )	26.58
Diameter of bow thruster: $D_{BT}$ (m)	2.5
Diameter of stern thruster: $D_{ST}$ (m)	2.5
Mass: $m$ (ton)	31,412
Longitudinal center of gravity: $x_G$ (m)	15.84
Transverse projected area: $A_T$ (m <sup>2</sup> )	213.55
Lateral projected area: $A_L$ (m <sup>2</sup> )	1150.50
Block coefficient: $C_b$	0.831

## 2.2. Mathematical Model of Maneuvering

In this section, the mathematical model of ship maneuvering is presented. In this study, the Mathematical Maneuvering Group model (MMG model) (Yasukawa and Yoshimura, 2015) is applied.

### 2.2.1. Subject Ship

The subject ship of this study is the same as previous (Maki et al., 2020a). The subject ship is VLCC M.V. *Esso Osaka*, a single-rudder and single-fixed pitch propeller ship. Although actual *Esso Osaka* does not have any side thruster, to achieve berthing without support from the tug, numerical bow thruster and stern thruster model were added. *Esso Osaka* was chosen because of its availability of the maneuvering model, while the actual ships operated on the subject ports shown on section 3.1 are passenger ferry and RORO cargo ship. These actual ships operated without the assistance of tug during berthing and unberthing and were equipped with side thrusters and a controllable pitch propeller. Although the size was a model scale in the previous study (Maki et al., 2020a), it was expanded to actual ship size. To be equivalent to the ships actually operated on the subject ports, the ship size was shrunken to  $L_{pp} = 150$  m while Original *Esso Osaka* is  $L_{pp} = 325$  m. The principal particulars of the subject ship are shown in Table 3.

### 2.2.2. MMG model

The 3-DoF equation of motion of MMG model is express as follows:

$$\begin{aligned}
 (m + m_x)\dot{u} - (m + m_y)v_m r - x_G m r^2 &= F_x \\
 (m + m_x)\dot{v}_m - (m + m_y)ur + x_G m \dot{r} &= F_y \\
 (I_{zz} + J_{zz} + x_G^2 m)\dot{r} - x_G m(\dot{v}_m + ur) &= M_N
 \end{aligned} \tag{17}$$

with

$$\begin{aligned}
 F_x &= X_H + X_P + X_R + X_A \\
 F_y &= Y_H + Y_P + Y_R + Y_{SS} + Y_A \\
 M_N &= N_H + N_P + N_R + N_{SS} + N_A .
 \end{aligned} \tag{18}$$

Since the MMG model decomposes the hydrodynamic force acting on the ship to sub-model for major components con-

sisting of the ship, the right-hand side of Eq. (18) represents the force or moment acting on each component of the ship; the subscripts H, P, R, A and SS denote the hull, the propeller, the rudder, the external forces by wind and the side thrusters, respectively. Each sub-model contains model coefficients to estimate force from input  $\mathbf{u}$  and state  $\mathbf{x}$ . The model coefficients, also known as hydrodynamic coefficients, are vessel-specific, and they may vary by the scale of the ship; due to the large discrepancy of the Reynolds number between a scale model for towing tank experiments and the actual ship. However, in this study, model coefficients obtained by scale model test ((Hachii, 2004; Kobayashi et al., 2002) were used, because the values for  $L_{pp} = 150$  m of *Esso Osaka* are unknown.

Choice of sub-model follows the previous research (Maki et al., 2020a), with several new additions. For the force acting on the hull, Yoshimura's unified model (Yoshimura et al., 2009) was applied. For the force induced by the propeller, the model is switched based on the operating condition of the propeller. For the propeller forward rotation ( $n_p \geq 0$ ), thrust force  $X_p$  expressed by standard MMG model (Yasukawa and Yoshimura, 2015). For the propeller reversal condition ( $n_p < 0$ ), propeller force and moment are modeled by a polynomial equation based on towing tank experiment (Hachii, 2004; Ueno et al., 2001). For the force induced by rudder, standard MMG model was applied for forwarding ( $u \geq 0$ ) condition and 4th quadrant operation ( $u < 0, n_p < 0$ ), Kitagawa's model (Kitagawa et al., 2015) for 3rd quadrant operation ( $u < 0, n_p \geq 0$ ). Refer Miyauchi et al. (2021) for the detail of the MMG model used in this paper.

Regarding the external force induced by wind disturbance, Fujiwara's regression formulae (Fujiwara et al., 1998) was used to estimate the wind pressure coefficients:

$$\begin{aligned} X_A &= (1/2)\rho_A U_A^2 A_T \cdot C_X \\ Y_A &= (1/2)\rho_A U_A^2 A_L \cdot C_Y \\ N_A &= (1/2)\rho_A U_A^2 A_L L_{OA} \cdot C_N \end{aligned} \quad (19)$$

where

$$\begin{aligned} C_X &= X_0 + X_1 \cos(2\pi - \gamma_A) + X_3 \cos 3(2\pi - \gamma_A) \\ &\quad + X_5 \cos 5(2\pi - \gamma_A) \\ C_Y &= Y_1 \sin(2\pi - \gamma_A) + Y_3 \sin 3(2\pi - \gamma_A) \\ &\quad + Y_5 \sin 5(2\pi - \gamma_A) \\ C_N &= N_1 \sin(2\pi - \gamma_A) + N_2 \sin 2(2\pi - \gamma_A) \\ &\quad + N_3 \sin 3(2\pi - \gamma_A) \end{aligned} \quad (20)$$

$\rho_A$  is the density of air,  $A_T$ ,  $A_L$ ,  $L_{OA}$  are the transverse projected area, the lateral projected area, and the overall length of the ship, respectively.  $X_i$ ,  $Y_i$ ,  $N_i$  are coefficients to express wind pressure coefficients derived by the regression formulae, which use geometric parameters of the ship as explanatory variables and based on wind tunnel experiment data of numerous scaled ship models.

For the side thruster model, Kobayashi's model (Kobayashi, 1988, 1990) was used, which follows

$$\begin{aligned} X_{ST} &= 0 \\ Y_{SS} &= (1 + a_{YSB} \cdot |\text{Fr}|) \cdot T_{BT} \\ &\quad + (1 + a_{YST} \cdot |\text{Fr}|) \cdot T_{ST} \\ N_{SS} &= (1 + a_{NSB} \cdot |\text{Fr}|) \cdot T_{BT} \cdot x_{BT} \\ &\quad + (1 + a_{NST} \cdot |\text{Fr}|) \cdot T_{ST} \cdot x_{ST} \\ T_{BT} &= \rho D_{BT}^4 n_{BT}^2 K_{TBT} \\ T_{ST} &= \rho D_{ST}^4 n_{ST}^2 K_{TST} \end{aligned} \quad (21)$$

Here,  $a_{YBT}$ ,  $a_{NBT}$ ,  $a_{YST}$ ,  $a_{NST}$  are the coefficients expressing the interaction between hull and thruster.  $x_{BT}$ ,  $x_{ST}$  are the longitudinal location of side thruster. In addition to the interaction effect, the thrust of side thrusters are cut-off when the longitudinal speed is larger than the threshold:  $|u| > u_{\text{threshold}}$ . The value of threshold  $u_{\text{threshold}} = 2.5722$  (m/s) is equivalent to 5 knots in this study.

## 3. Computation Results

### 3.1. Port Geometry

Two ports in Japanese waters were selected for computation; Port of *Nanko* at Osaka bay and the port of *Ariake* at Tokyo bay. Nanko is the primary port in this study, while Ariake is alternate to verify the applicability to arbitrary port geometry of the present method. Overview of ports is shown in Fig. 4 and Fig. 5. These figures also show the start points and the endpoints of berthing. Table 4 and Table 5 show the detailed value of  $\mathbf{x}_{\text{int}}$  and  $\mathbf{x}_{\text{des}}$  of computation. As stated in the section 2, the origin of  $O_0 - x_0 y_0$  coordinates system is set to the endpoint for berthing and the start point for unberthing. The start point of berthing was set just outside the breakwaters of the port. This is because, outside the breakwater, the spatial constrain is not severe as inside; hence the appropriate collision avoidance method might differ. The endpoint was set at the point which perpendicular distance is 40 m from berth wall; Approximately 1.0  $B$  from the broadside of the ship. The berthing condition is the starboard side, head out at Nanko and port side, head out at Ariake. Note that the obstacle polygons include certain water surfaces at the vicinity of the breakwater as a restricted area.

Both ports have characteristics to make berthing and unberthing difficult: dead end, confined berth which ship necessary to turn 180 degrees, require several course change during navigation, and obstacle landfills that exclude the intended berth. The case of Nanko also has a moored vessel near the berthing point as an obstacle. Generally, the ship must comply with the international and local traffic rules; the ship must navigate in the designated passage in a port (for the regulation on the port of Nanko, see The Harbor Information Center for the Security of Ship Navigation (2020)). However, in this study, regulatory requirements such as passage and fairway are not considered.

The minimum passage width  $W$ , which is the design parameter of domain boundary vertices, are 3.08  $L_{pp}$  for Nanko and 2.40  $L_{pp}$  for Ariake, respectively.

**Table 4**  
Computation condition of port of Nanko

Parameter	Value
Condition	Berthing
$\mathbf{x}_{\text{int}}$	$(-598.7 \text{ m}, 8.0 \text{ kn}, -1845.2 \text{ m}, 0.0 \text{ m/s}, 132^\circ, 0.0^\circ/\text{s})^T$
$\mathbf{x}_{\text{des}}$	$(0.0\text{m}, 0.0\text{kn}, 0.0\text{m}, 0.0\text{m/s}, 227^\circ, 0.0^\circ/\text{s})^T$
Condition	UnBerthing
$\mathbf{x}_{\text{int}}$	$(0.0 \text{ m}, 0.0 \text{ kn}, 0.0 \text{ m}, 0.0 \text{ m/s}, 227^\circ, 0.0^\circ/\text{s})^T$
$\mathbf{x}_{\text{des}}$	$(-598.7 \text{ m}, 6.0 \text{ kn}, -1845.2 \text{ m}, 0.0 \text{ m/s}, 312^\circ, 0.0^\circ/\text{s})^T$

**Table 5**  
Computation condition of port of Ariake

Parameter	Value
Condition	Berthing
$\mathbf{x}_{\text{int}}$	$(-891.3 \text{ m}, 8.0 \text{ kn}, 3317.5 \text{ m}, 0.0 \text{ m/s}, 326^\circ, 0.0^\circ/\text{s})^T$
$\mathbf{x}_{\text{des}}$	$(0.0\text{m}, 0.0\text{kn}, 0.0\text{m}, 0.0\text{m/s}, 146^\circ, 0.0^\circ/\text{s})^T$
Condition	UnBerthing
$\mathbf{x}_{\text{int}}$	$(0.0 \text{ m}, 0.0 \text{ kn}, 0.0 \text{ m}, 0.0 \text{ m/s}, 146^\circ, 0.0^\circ/\text{s})^T$
$\mathbf{x}_{\text{des}}$	$(-891.3 \text{ m}, 6.0 \text{ kn}, -3317.5 \text{ m}, 0.0 \text{ m/s}, 146^\circ, 0.0^\circ/\text{s})^T$

### 3.2. Berthing and Unberthing Results with proposed ship domain and collision avoidance algorithm

The trajectory planning of berthing and unberthing are conducted with newly introduced objective function including collision avoidance to the polygonal constraints on the port for Nanko. The convergence process in the optimization is shown in Fig. 6. The upper-left shows the best objective function  $J$  at each iteration. The upper-right shows the difference of  $J$  at each iteration and the minimum value of  $J$  through the optimization process. The lower-left and lower-right show the square root of the eigenvalue of the covariance matrix and the square root of the diagonal elements of the covariance matrix during the process, respectively. As stated in Maki et al. (2020b), the square root of each eigenvalue represents the axis length of the equidensity ellipsoid, whereas the square root of each diagonal element stands for the standard deviation in each coordinate. From the upper two sub-figures on Fig. 6,  $J$  shows impulse-like increases caused by the restart of CMA-ES. By using the restart strategy, CMA-ES let the  $J$  converge to several different local minima and choose the best solution from those. In the case of Fig. 6, the optimum solution is obtained at the 94000th iteration. In general, the convergence speed will vary by the computation conditions. However, the maximum iteration number of optimization processes was set to  $3 \times 10^5$  based on the convergence of Fig. 6, which occur several restarting and obtain local minima.

Since CMA-ES is based on a stochastic method, results will differ by the random seed. Table 6 show the  $t_f$ ,  $J$  and  $C$  of 10 independent trials on berthing computation of Nanko without wind disturbance. From the table, we can find the values of  $C$  are zero for all 10 trails. This means, not only collision occurred, but also berthing was conducted with sufficient distance to obstacle by maintaining ship domain. With the newly introduced collision avoidance algorithm,

collision avoidance to the obstacle of realistic port geometry was successfully achieved.

Fig. 7 shows the obtained control input  $\mathbf{u}(t)$  and state  $\mathbf{x}(t)$  achieved by the optimal  $\mathbf{u}(t)$  on berthing of Nanko without wind disturbance;  $U_T = 0$ . Note that if  $u > u_{\text{threshold}}$ , which means thrust of side thrusters are zero, shown as  $n_{BT} = 0$  and  $n_{ST} = 0$  in the figure. The figure indicates that the optimization on trajectory planning with the new collision avoidance algorithm works well; the ship has reached the berthing point while avoiding the static obstacles with sufficient distance. Fig. 8 shows the terminal phase of the same berthing result with Fig. 7; Trajectory and control input are shown only for times when the Euclidean distance between midship and berthing point is less than  $2 L_{pp}$ . In Fig. 7 and 8, the light blue ellipses around the ship are ship domain, which shown from  $t = 0$  to  $t = t_f$  at the intervals of 200 seconds. Fig. 8 also shows the domain boundary vertices themselves. As shown in Maki et al. (2020b), the subject ship tended to turn starboard while propeller reversal. It seems the CMA-ES found the solution which uses the characteristic on the reverse maneuvering of the subject ship to stop within the minimum time.

Fig.9 shows the result of the unberthing computation. Same as berthing, CMA-ES with the proposed collision avoidance algorithm can obtain resalable trajectory and control inputs.

Table7 shows the difference between the desired and the obtained end state:  $\mathbf{x}_{\text{des}} - \mathbf{x}(t_f)$  and  $t_f$  for both of berthing and unberthing. For the berthing,  $\mathbf{x}(t_f)$  just fits within the  $\mathbf{x}_{\text{tol}}$ . This is because objective function did not change when  $\mathbf{x}(t_f)$  was within the range of  $\mathbf{x}_{\text{tol}}$ , while CMA-ES tried to optimize by shortening the  $t_f$ . Meanwhile, in the unberthing computation,  $x_{\text{des},2} - x_2(t_f) < 0$  which means the  $\mathbf{u}(t_f)$  is faster than the desired exit speed, while other state satisfy  $\mathbf{x}_{\text{tol}}$ .

**Table 6**

 Statistical analysis data for  $J$  and  $t_f$  in 10 trials

: Minimum, Maximum, Quartiles, Mean, and Standard deviation.							
	min	max	$Q_1$	$Q_2$	$Q_3$	Mean	$\sigma$
$t_f$	1081.6	1177.1	1086.5	1098.2	1103.4	1106.0	29.3
$J$	18.077	19.673	18.159	18.355	18.407	18.484	0.490
$w_c \cdot C$	0.0	0.0	0.0	0.0	0.0	0.0	0.0

**Table 7**

Computation results of berthing and unberthing.

parameter	value
Condition	Nanko, berthing, $U_T = 0$
$\mathbf{x}_{des,i} - \mathbf{x}_i(t_f)$	(1.0m, 0.1m/s, -1.0m, -0.1m/s, 1.0°, -0.0764°/s) <sup>T</sup>
$t_f(s)$	1177.1
Condition	Nanko, unberthing, $U_T = 0$
$\mathbf{x}_{des,i} - \mathbf{x}_i(t_f)$	(1.0m, -0.2m/s, -1.0m, 0.02m/s, -1.0°, -0.0343°/s) <sup>T</sup>
$t_f(s)$	994.0

### 3.3. Result with Wind Disturbance

Generally, during the berthing and unberthing, the wind disturbance makes it difficult to control a vessel. Hence, the effect of wind must be included in the optimization of trajectory planning. Moreover, the wind has a critical effect on control a ship at the terminal phase of berthing because the thrusts of actuators are kept low, and the distance to berth is small while the ship drifted by the wind. Obviously, the wind speed and direction are unsteady, and instantaneous velocity can only be described by stochastic approach. Hence, it is not appropriate to implement unsteady wind directly to optimization because CMA-ES would optimize while knowing the time series of instantaneous wind due to its iterative process. Nevertheless, including *steady* wind disturbance is meaningful because considering severe conditions by wind disturbance, the obtained trajectory will be a more generous one that takes into account the limits of actuators. In addition to that, by increasing the wind speed, we can find the nominal wind speed limit of a certain ship and spatial constraints of the port.

Under the ideas discussed above, calculations with wind disturbance were conducted for both berthing and unberthing at Nanko. Fig.10, 11 show the berthing and unberthing results under wind disturbance of  $\omega = (137^\circ, 15 \text{ m/s})$ ; the true wind direction  $\gamma_T$  is perpendicular to the berth, which pushes the ship towards berth wall. From the figures, we can see that the CMA-ES can obtain a reasonable trajectory even under the wind disturbance when the actuator is capable enough.

### 3.4. Verification on Different Port Geometry

To show that the proposed method is applicable to multiple ports, it is necessary to verify the method on ports other than Nanko, used in the previous section. Ariake has the same spatial constraints characteristics while the travel distance is slightly longer than Nanko and berthing to the port side. Fig.12 and Fig.13 show the results, which seem reasonable. From the results, we can see that the proposed method

is appreciable to different kinds of ports.

### 3.5. Trajectory Planning Optimization with Waypoints

As shown in the previous section, the proposed method was able to find an appropriate trajectory even under the constraint of complex port geometry. On the other hand, it was found that the proposed method does not provide a reasonable solution within the iteration limit when the ship starts from a position far from the breakwaters at the entrance of the port and the initial heading does not point to the entrance of the port. Fig. 14 shows one of the results of such cases, only the local minimum solution that the  $t_f$  ends early while advance speed  $u$  remain large, was obtained. We assumed that this was because: solution exploration not proceed to solutions that navigate to the entrance of port, because the gradient of increasing  $J$  occur around the solution toward the opening of the breakwater, due to the small choice of control inputs which can enter to the opening of the breakwater, and surrounding solutions of the favorable solution have significantly large  $J$  caused by penalty of collision to breakwaters; a solution that goes straight forward from the initial heading is likely to occur, even if the rudder angle is searched randomly. This is because to change the course of a ship, the rudder angle needs to maintain a certain period until the maneuver develops.

To obtain reasonable solutions of trajectory planning regardless of choice of the initial condition, we tried to generate favorable gradient of the objective function of Eq. (2) when searching the solution around the entrance of port, by including the waypoint portion to  $J$ . The  $J$  shown on Eq. (2) was modified to include the component of waypoints  $J_{WP}$ :

$$J = (J_1 + J_{WP}) \cdot t_f + w_c C, \quad (22)$$

where

$$J_1 = \sum_{i=1}^6 w_{dim,i} \left( x_{tol,i}^2 \mathbf{1}_{\{|x_{des,i} - x_i(t_f)| \leq x_{tol,i}\}} \right)$$



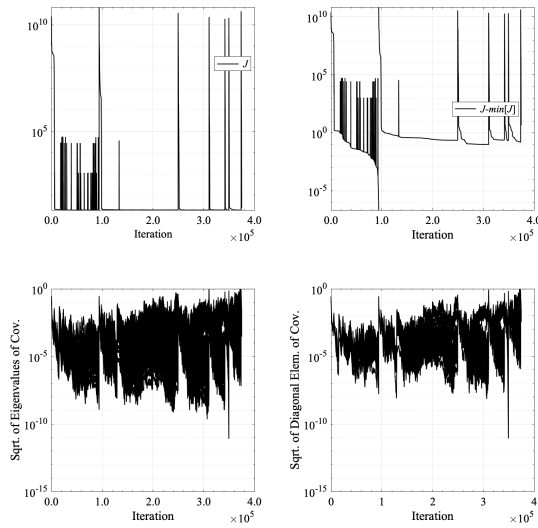


Fig. 6: Optimization process of CMA-ES.

input on real port geometry. Our proposed method can directly apply to the arbitrary spatial constraints while similar research mentioned in section 1.1 (Martinsen et al., 2020; Bitar et al., 2020; Bergman et al., 2020) have adopted the two-stage method; discrete the continuous state space to apply graph search which obtains an initial guess. The present method can handle the comprehensive ship's dynamics while graph search method can only address purely geometric space or limited way of ship dynamics. In addition, the present method varies the ship domain with speed which is natural for navigators' sense, while similar research (Bitar et al., 2020; Bergman et al., 2020) have only adopted to circular safety region around the ship with a constant radius.

Obtained trajectory and control can serve as a reference to the tracking control of berthing although the present method can not directly apply to the berthing control because of the computational requirement of the optimization process, which is due to the iteration. In the case of optimization of control method which applies finite prediction horizon such as model predictive control could be unstable when the prediction horizon gets longer, however by offering predefined trajectory as a reference those obtained by the present method, which is optimized collision-free trajectory, prediction horizon can be taken shorter. Besides, the obtained result can also use to estimate the limit of actuator capability, which could maintain collision-free trajectory on certain wind and port geometry by testing on various wind conditions.

Regarding the potential future work, by improving two essential factors of trajectory planning, our work can add value as a reference trajectory; safety and optimization. From the safety perspective, the mathematical model of ship maneuver was assumed accurate enough. However, mathematical modeling of berthing maneuver itself still remains as research topic due to: the complexity and non-linearity of

berthing motion; scale effect on hydrodynamic coefficients; and effect of shallow water and a sidewall. To negotiate the uncertainty of motion estimation caused by those factors, the robust optimization method is one option for improvement. In robust optimization, the range of possible range of uncertainty on input data is set in advance, and optimization is performed on the input data, which gives the worst result (Ben-Tal et al., 2009). From the optimization perspective, on the other hand, the practical berthing process is not just a single objective problem of time; optimization of berthing is a multi-objective optimization problem with the trade-off between time, energy consumption, and ride quality especially for passenger vessels. It is better to consider optimizing the berthing (and unberthing) trajectory as a multi-objective optimization problem that minimizes several factors simultaneously.

## 5. Conclusion

To achieve optimization of trajectory planning of berthing and unberthing of a ship at a real port, it is necessary to consider the spatial constraints, such as berths, breakwaters, buoys, or anchoring vessels. The novel collision avoidance algorithm was proposed, representing the spatial obstacles as polygons and includes a ship domain to maintain the sufficient distance to obstacles. The proposed ship domain consists of domain boundary vertices that discretize the ellipse shape of the ship domain with a uniform argument angle, and the size of the ship domain changes with ship's speed, which is based on the navigators' knowledge and experience.

Optimization of trajectory planning for two existing ports, Nanko and Ariake, were conducted by using the proposed collision avoidance algorithm with CMA-ES and the MMG model. By introducing the proposed collision avoidance algorithm, collision-free time-optimized control inputs and trajectories were obtained. The effect of wind disturbance was also considered. By considering the wind force, the obtained trajectory will be more robust that considers the limits of actuators. Additionally, optimization with waypoints also shown in this study. Including the waypoints to objective function makes it more robust to the choice of the initial location of berthing simulation. Although its long computation time due to the iteration, it should be noted that the present method requires only the mathematical model of ship maneuver, a start point, an end point, polygons of spatial constraints, and waypoints, if necessary, to obtain an optimized trajectory at the real port. The optimized trajectory can serve as a predefined reference to the real-time tracking control of berthing and unberthing.

## CRedit authorship contribution statement

**Yoshiki Miyauchi:** Methodology, Software, Writing - original draft, visualization. **Ryohei Sawada:** Methodology, Writing - review & editing. **Youhei Akimoto:** Software, Writing - review & editing. **Naoya Umeda:** Supervi-

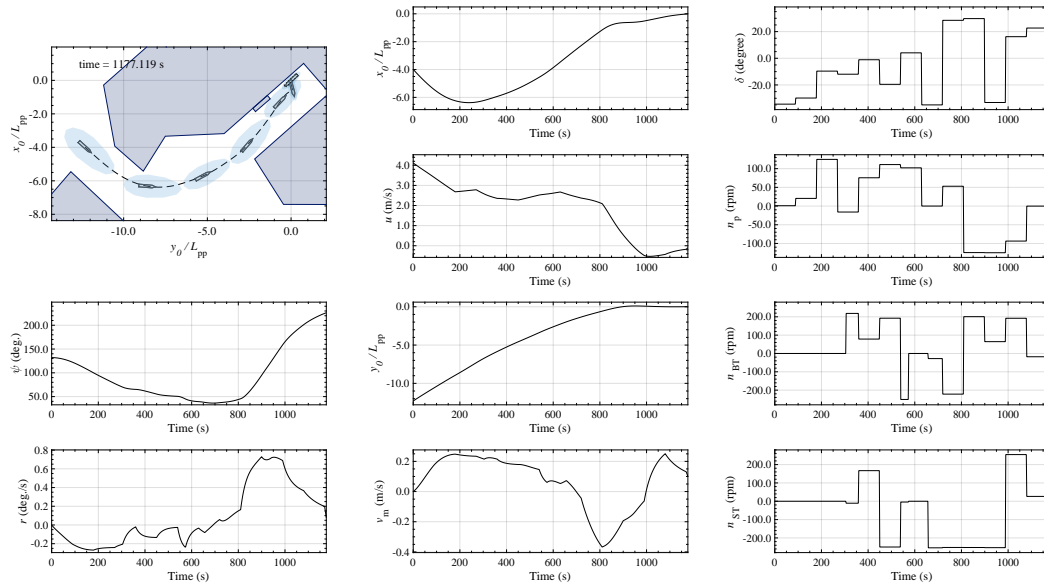


**Fig. 7:** Optimized control inputs and achieved state of berthing on port of Nanko. Ellipses shown in light blue on figure of trajectory at upper left are the ship domains used in collision avoidance function.

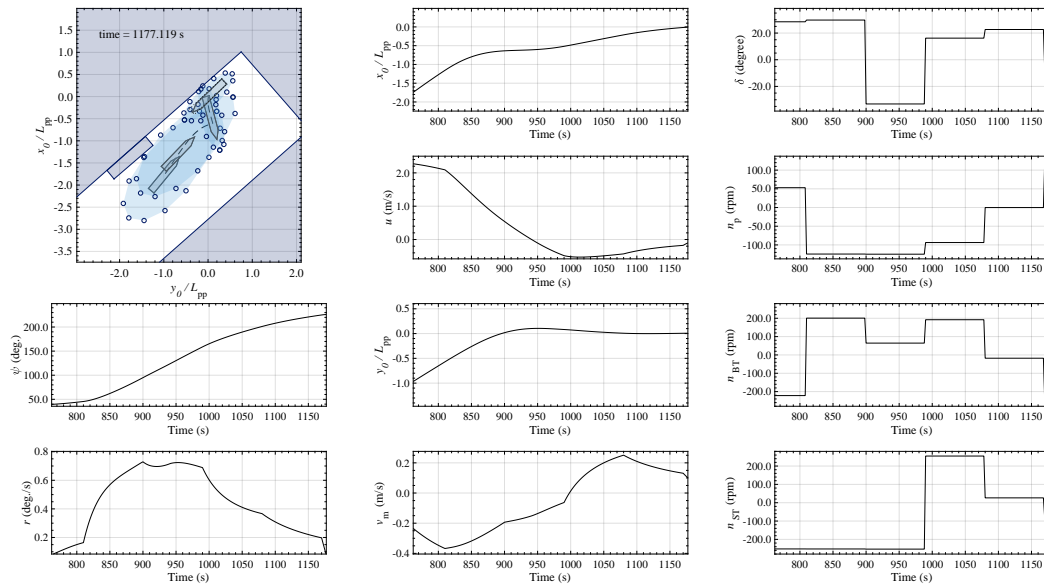


**Fig. 8:** Terminal phase of Fig.7 which of the Euclidean distance to berthing point is smaller than  $2 L_{pp}$ . Blue circles on the upper left figure are the collision avoidance points.

tion, Funding acquisition. **Atsuo Maki:** Conceptualization, Writing - review & editing.

### Declaration of competing interest

The authors declare that they have no known competing financial interests or personal relationships that could have appeared to influence the work reported in this paper.

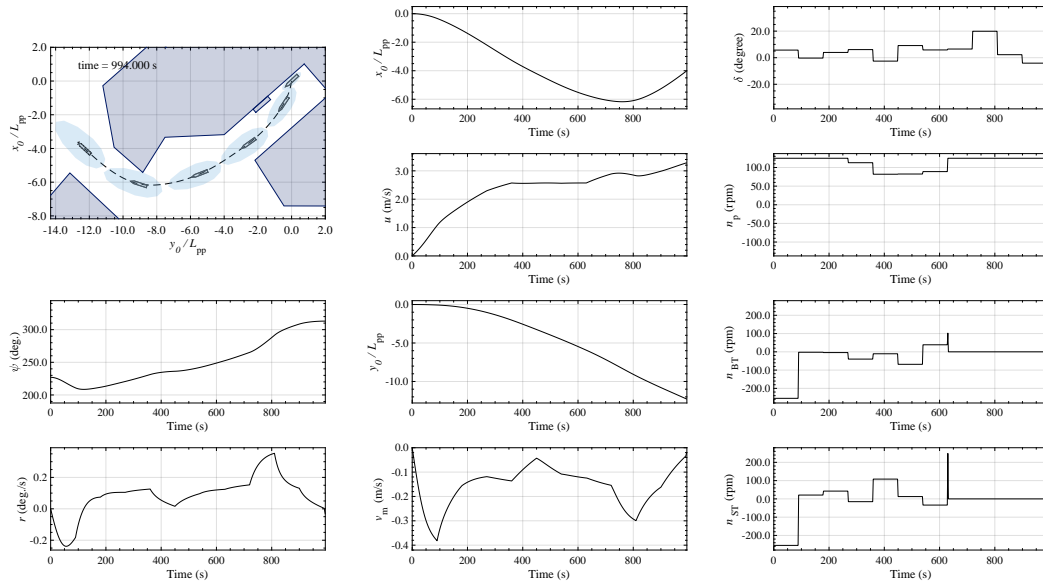


**Fig. 9:** Optimized control inputs and achieved state of unberthing on port of Nanko. Ellipse shown in light blue on figure of trajectory at upper left is the ship domain used in collision avoidance function.

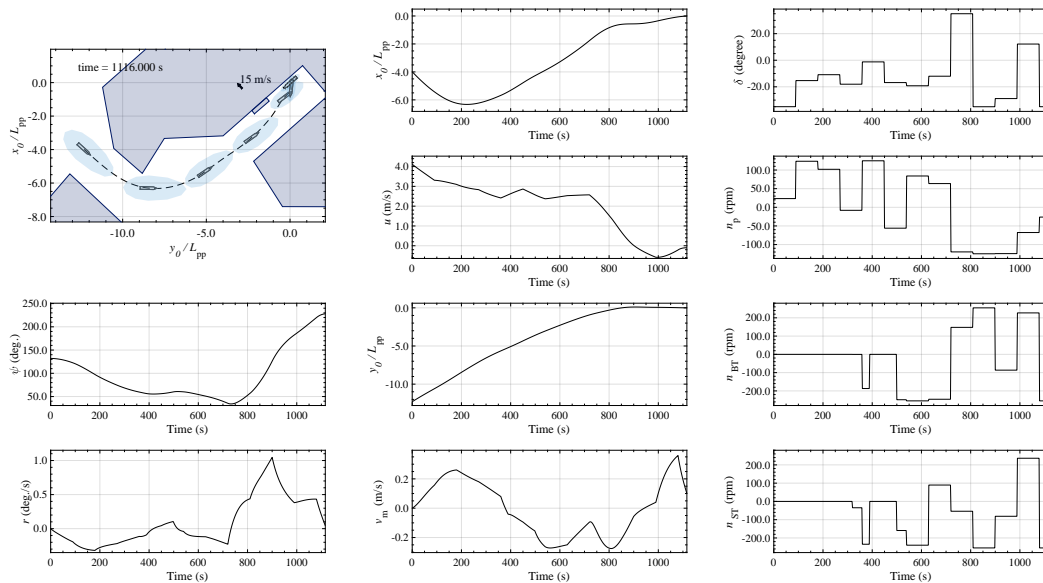


**Fig. 10:** Optimized control inputs and achieved state of berthing on port of Nanko. With wind disturbance  $U_T = 15$  m/s

## Acknowledgment

This study was supported by a Grant-in-Aid for Scientific Research from the Japan Society for Promotion of Science (JSPS KAKENHI Grant #19K04858). The study also received assistance from JFY2018 Fundamental Research Developing Association for Shipbuilding and Off-

shore (REDAS) in Japan.

## References

- Ahmed, Y.A., 2015. Automatic Berthing Control Practically Applicable under Wind Disturbances. Ph.D. thesis. Osaka University.
- Amendola, J., Miura, L.S., Costa, A.H., Cozman, F.G., Tannuri, E.A., 2020. Navigation in restricted channels under environmental conditions: Fast-

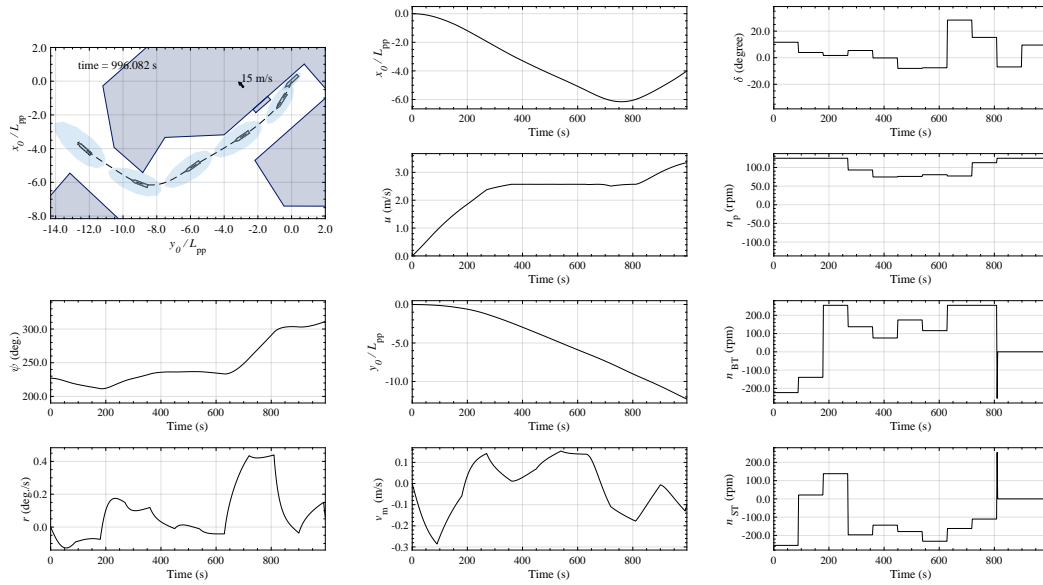


Fig. 11: Optimized control inputs and achieved state of unberthing on port of Nanko. With wind disturbance  $U_T = 15$  m/s

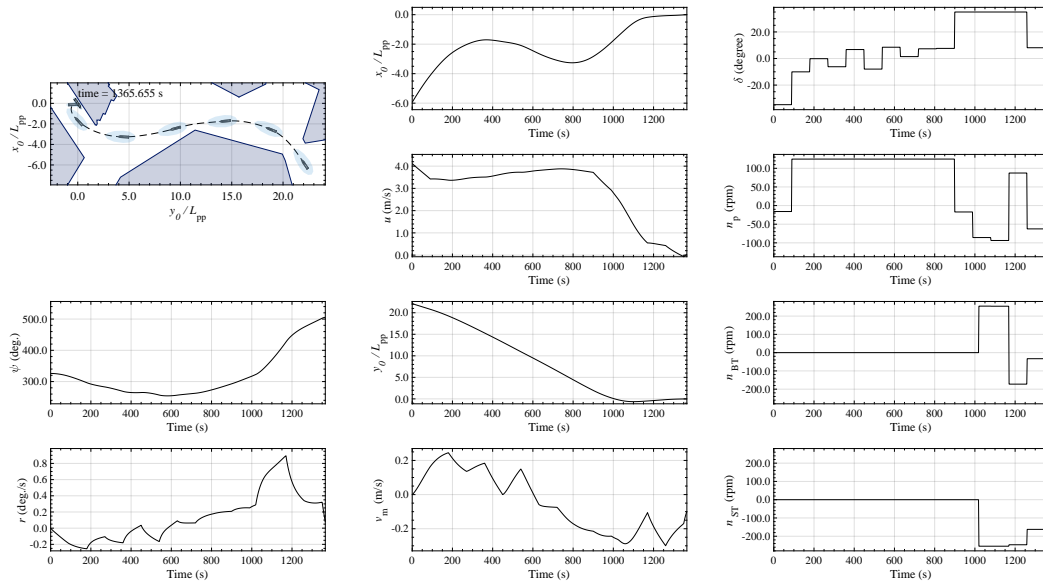


Fig. 12: Optimized control inputs and achieved state of berthing on port of Ariake. Without the wind disturbance.

time simulation by asynchronous deep reinforcement learning. IEEE Access 8, 149199–149213. doi:10.1109/ACCESS.2020.3015661.

Auger, A., Hansen, N., 2005. A restart cma evolution strategy with increasing population size, in: 2005 IEEE Congress on Evolutionary Computation, IEEE. pp. 1769–1776. URL: <http://ieeexplore.ieee.org/document/1554902/>, doi:10.1109/CEC.2005.1554902.

Ben-Tal, A., Ghaoui, L., Nemirovski, A., 2009. Robust Optimization. Princeton Series in Applied Mathematics, Princeton University Press. URL: <https://books.google.co.jp/books?id=DttjR7IppjUEC>.

Bergman, K., Ljungqvist, O., Linder, J., Axehill, D., 2020. An Optimization-Based Motion Planner for Autonomous Maneuvering of Marine Vessels in Complex Environments, in: 2020 59th IEEE Conference on Decision and Control (CDC), IEEE. pp. 5283–5290. URL: <https://ieeexplore.ieee.org/document/9303746/http://arxiv.org/abs/2012.12145>, doi:10.1109/CDC42340.2020.9303746, arXiv:2005.02674.

Bitar, G., Martinsen, A.B., Lekkas, A.M., Breivik, M., 2020. Two-stage optimized trajectory planning for asvs under polygonal ob-

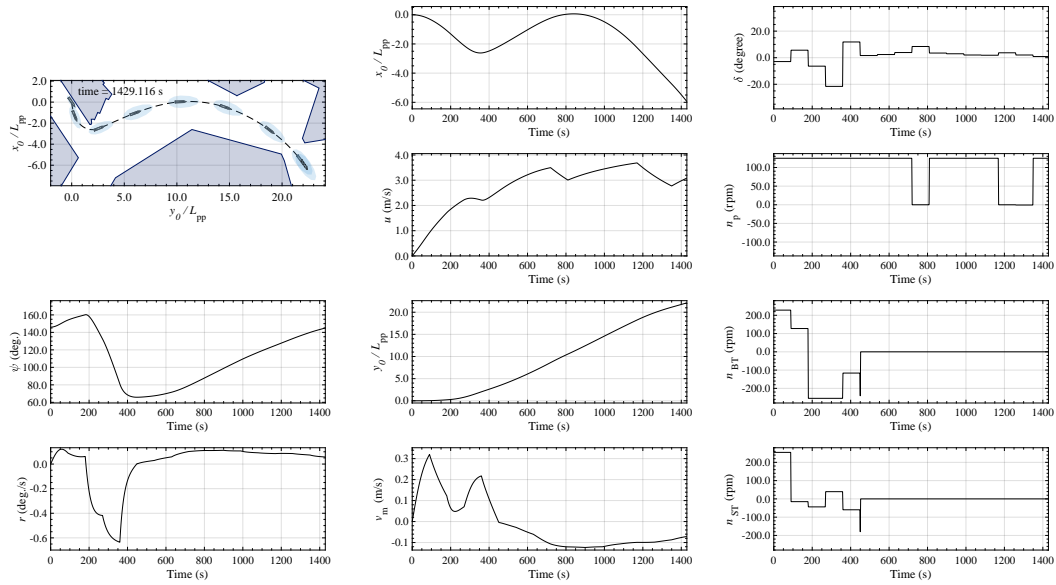


Fig. 13: Optimized control inputs and achieved state of unberthing on port of Ariake. Without the wind disturbance.

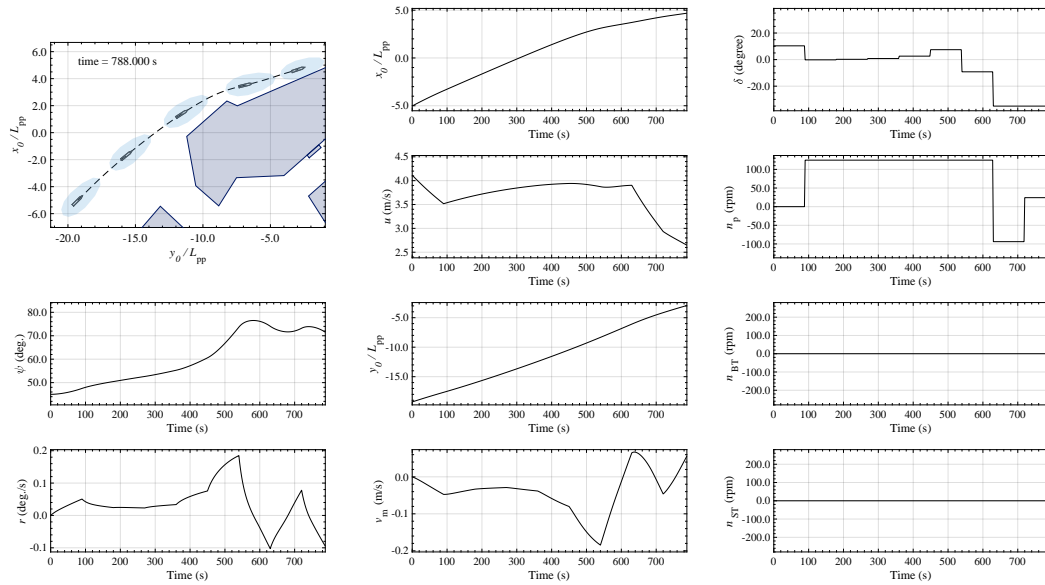


Fig. 14: Example of unfavorable solution at Nanko. The trajectory did not enter the opening of breakwater to enter the berth.

stacle constraints: Theory and experiments. IEEE Access 8, 199953–199969. URL: <https://www.maritime-executive.com/article/rolls-royce-and-wartsila->, doi:10.1109/access.2020.3035256.

Fujii, Y., Tanaka, K., 1971. Traffic capacity. Journal of Navigation 24, 543–552. URL: [https://www.cambridge.org/core/product/identifier/S037346330022384/type/journal\\_article](https://www.cambridge.org/core/product/identifier/S037346330022384/type/journal_article), doi:10.1017/S0373463300022384.

Fujiwara, T., Ueno, M., Nimura, T., 1998. Estimation of wind forces and moments acting on ships. Journal of the Society of Naval Architects of Japan 1998, 77–90. URL: <http://joi.jlc.jst.go.jp/JST.Journalarchive/jjasnaoe1968/1998.77?from=CrossRef>, doi:10.2534/jjasnaoe1968.1998.77.

Goodwin, E.M., 1975. A statistical study of ship domains. Journal of Navigation 28, 328–344. doi:10.1017/S0373463300041230.

Hachii, T., 2004. The prediction of manoeuvring motion on ships with low speed using standard MMG model. Master’s thesis. Osaka University.

Hansen, M.G., Jensen, T.K., Lehn-Schiøler, T., Melchior, K., Rasmussen, F.M., Ennemark, F., 2013. Empirical ship domain based on ais data.



Fig. 15: way point of port of Nanko

- Journal of Navigation 66, 931–940. URL: [https://www.cambridge.org/core/product/identifier/S0373463313000489/type/journal\\_article](https://www.cambridge.org/core/product/identifier/S0373463313000489/type/journal_article), doi:10.1017/S0373463313000489.
- Hansen, N., 2006. *The CMA Evolution Strategy: A Comparing Review*. Springer Berlin Heidelberg, Berlin, Heidelberg. pp. 75–102. URL: [https://doi.org/10.1007/3-540-32494-1\\_4](https://doi.org/10.1007/3-540-32494-1_4), doi:10.1007/3-540-32494-1\_4.
- Hasegawa, K., Kitera, K., 1993. Mathematical model of manoeuvrability at low advance speed and its application to berthing control, in: 2nd Japan-Korea Joint Workshop on Ship and Marine Hydrodynamics, pp. 311–321.
- Inoue, K., Usami, S., Shibata, T., 1994. Modelling of mariners' senses on minimum passing distance between ships in harbour. *The Journal of Japan Institute of Navigation* 90, 297–306. doi:10.9749/jin.90.297.
- Jensen, T.K., Hansen, M.G., Lehn-Schiøler, T., Melchild, K., Rasmussen, F.M., Ennemark, F., 2013. Free flow–efficiency of a one-way traffic lane between two pylons. *Journal of Navigation* 66, 941–951. URL: <https://doi.org/10.1017/S0373463313000362>[https://www.cambridge.org/core/product/identifier/S0373463313000362/type/journal\\_article](https://www.cambridge.org/core/product/identifier/S0373463313000362/type/journal_article), doi:10.1017/S0373463313000362.
- Kitagawa, Y., Tsukada, Y., Miyazaki, H., 2015. 2015-sgs1-1 a study on mathematical models of propeller and rudder under maneuvering with propeller reverse rotation. *Conference Proceedings The Japan Society of Naval Architects and Ocean Engineers* 20, 117–120. doi:10.14856/conf.20.0\_117.
- Kobayashi, E., 1990. Manoeuvring simulation at low speed for a ship with twin screw, rudders and thrusters. *MARSIM and ICSM 90, Intl. Conference, Marine Simulation and Ship Manoeuvrability*.
- Kobayashi, H., Blok, J., Barr, R., Kim, Y.S., Nowicki, J., 2002. The specialist committee on esso osaka final report and recommendations to the 23rd ittc. *23rd International Towing Tank Conference II*, 581–743.
- Kobayashi, M., 1988. A simulation study on ship manoeuvrability at low speeds. Akishima Laboratory, Ocean Engineering Research Section, Mitsubishi Heavy Industries Ltd. Published in: Mitsubishi Technical Bulletin No. 180.
- Maki, A., Akimoto, Y., Naoya, U., 2020a. Application of optimal control theory based on the evolution strategy (cma-es) to automatic berthing (part: 2). *Journal of Marine Science and Technology (Japan)* doi:10.1007/s00773-020-00774-x.
- Maki, A., Sakamoto, N., Akimoto, Y., Nishikawa, H., Umeda, N., 2020b. Application of optimal control theory based on the evolution strategy (cma-es) to automatic berthing. *Journal of Marine Science and Technology* 25, 221–233. URL: <https://doi.org/10.1007/s00773-019-00642-3><http://link.springer.com/10.1007/s00773-019-00642-3>, doi:10.1007/s00773-019-00642-3.
- Martinsen, A.B., Lekkas, A.M., Gros, S., 2019. Autonomous docking using direct optimal control. *IFAC-PapersOnLine* 52, 97–102. doi:10.1016/j.ifacol.2019.12.290.
- Martinsen, A.B., Lekkas, A.M., Gros, S., 2020. Optimal model-based trajectory planning with static polygonal constraints. *arXiv preprint arXiv:https://arxiv.org/abs/2010.14428*.
- Miyauchi, Y., Richman, D., Maki, A., Umeda, N., Akimoto, Y., 2021. Coefficient exploration of maneuvering model for automatic docking / berthing using cma-es. *Journal of Marine Science and Technology (to be submitted)*.
- Murakami, K., Takenobu, M., Miyata, T., Yoneyama, H., 2015. *Fundamental Analysis on the Characteristics of Berthing Velocity of Ships For the Design of Port Facilities*. Technical Report. TECHNICAL NOTE of National Institute for Land and Infrastructure Management.
- Pietrzykowski, Z., 2008. Ship's fuzzy domain – a criterion for navigational safety in narrow fairways. *Journal of Navigation* 61, 499–514. URL: [https://www.cambridge.org/core/product/identifier/S0373463308004682/type/journal\\_article](https://www.cambridge.org/core/product/identifier/S0373463308004682/type/journal_article), doi:10.1017/S0373463308004682.
- Roubos, A., Groenewegen, L., Peters, D.J., 2017. Berthing velocity of large seagoing vessels in the port of rotterdam. *Marine Structures* 51, 202–219. doi:10.1016/j.marstruc.2016.10.011.
- Sakamoto, N., Akimoto, Y., 2017. Modified box constraint handling for the covariance matrix adaptation evolution strategy, in: *Proceedings of the Genetic and Evolutionary Computation Conference Companion, Association for Computing Machinery, New York, NY, USA*. p. 183–184. URL: <https://doi.org/10.1145/3067695.3075986>, doi:10.1145/3067695.3075986.
- Serigstad, E., Eriksen, B.O.H., Breivik, M., 2018. Hybrid collision avoidance for autonomous surface vehicles. *IFAC-PapersOnLine* 51, 1–7. URL: <https://linkinghub.elsevier.com/retrieve/pii/S2405896318321499>, doi:10.1016/j.ifacol.2018.09.460.
- Seta, H., Inoue, K., USsui, H., 2004. Supporting information for safe ship handling based on the concept of potential area of water. *The Journal of Japan Institute of Navigation* 111, 63–69. URL: [https://www.jstage.jst.go.jp/article/jin/111/0/111\\_KJ0000469669/\\_article/-char/ja](https://www.jstage.jst.go.jp/article/jin/111/0/111_KJ0000469669/_article/-char/ja), doi:10.9749/jin.111.63.
- Szlapczynski, R., Szlapczynska, J., 2017. Review of ship safety domains: Models and applications. *Ocean Engineering* 145, 277–289. doi:10.1016/j.oceaneng.2017.09.020.
- The Harbor Information Center for the Security of Ship Navigation, 2020. *Port of Osaka Entrance and Departure Manual*. Revised ed., Osaka ports and harbors bureau.
- Ueno, M., Nimura, T., Miyazaki, H., Fujiwara, T., Nonaka, K., Yabuki, H., 2001. Model experiment and sea trial for investigating manoeuvrability of a training ship. *Journal of the Society of Naval Architects of Japan* 2001, 71–80. URL: <http://joi.jlc.jst.go.jp/JST.Journalarchive/jjasnaoe/1968/2001.71?from=CrossRef>, doi:10.2534/jjasnaoe1968.2001.71.
- Vagale, A., Oucheikh, R., Bye, R.T., Osen, O.L., Fossen, T.I., Oucheikh, R., Osen, O.L., Fossen, T.I., 2021. Path planning and collision avoidance for autonomous surface vehicles I: a review. *Journal of Marine Science and Technology* URL: <https://doi.org/10.1007/s00773-020-00787-6><http://link.springer.com/10.1007/s00773-020-00787-6>, doi:10.1007/s00773-020-00787-6.
- Wang, Y., Chin, H.C., 2016. An empirically-calibrated ship domain as a safety criterion for navigation in confined waters. *Journal of Navigation* 69, 257–276. URL: [https://www.cambridge.org/core/product/identifier/S0373463315000533/type/journal\\_article](https://www.cambridge.org/core/product/identifier/S0373463315000533/type/journal_article), doi:10.1017/S0373463315000533.
- Yamanouchi, H., Fujii, Y., 1972. On the hard core of the effective domain in yokohama port. *NAVIGATION* 38, 56–57. doi:10.18949/jinnavig.38.0\_56.
- Yasukawa, H., Yoshimura, Y., 2015. Introduction of mmg standard method for ship maneuvering predictions. *Journal of Marine Science and Technology (Japan)* 20, 37–52. doi:10.1007/s00773-014-0293-y.
- Yoshimura, Y., Nakao, I., Ishibashi, A., 2009. Unified mathematical model for ocean and harbour manoeuvring, in: *Proceedings of MARSIM2009*, pp. 116–124. URL: <http://hdl.handle.net/2115/42969>.

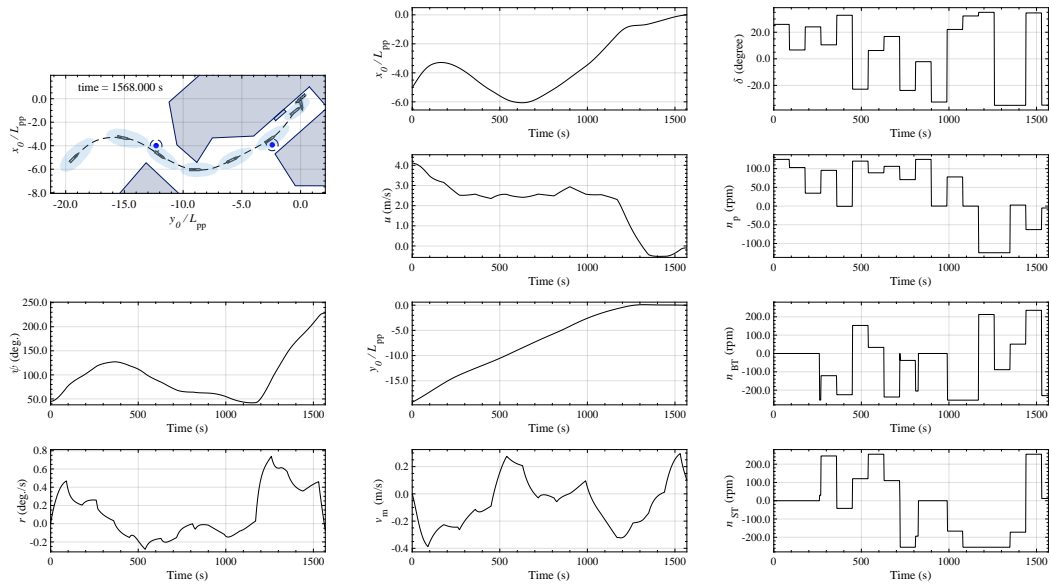


Fig. 16: Computation with way points at Nanko. blue dashed circle shows the way point with tolerance distance.